High Apparent Dielectric Constants in the Interior of a Protein Reflect Water Penetration

John J. Dwyer,* Apostolos G. Gittis,* Daniel A. Karp,* Eaton E. Lattman,* Daniel S. Spencer,† Wesley E. Stites,† and Bertrand García-Moreno E.*

*Department of Biophysics, Johns Hopkins University, Baltimore, Maryland 21218, and †Department of Chemistry and Biochemistry, University of Arkansas, Fayetteville, Arkansas 72701 USA

ABSTRACT A glutamic acid was buried in the hydrophobic core of staphylococcal nuclease by replacement of Val-66. Its pK_a was measured with equilibrium thermodynamic methods. It was 4.3 units higher than the pK_a of Glu in water. This increase was comparable to the ΔpK_a of 4.9 units measured previously for a lysine buried at the same location. According to the Born formalism these ΔpK_a are energetically equivalent to the transfer of a charged group from water to a medium of dielectric constant of 12. In contrast, the static dielectric constants of dry protein powders range from 2 to 4. In the crystallographic structure of the V66E mutant, a chain of water molecules was seen that hydrates the buried Glu-66 and links it with bulk solvent. The buried water molecules have never previously been detected in >20 structures of nuclease. The structure and the measured energetics constitute compelling and unprecedented experimental evidence that solvent penetration can contribute significantly to the high apparent polarizability inside proteins. To improve structure-based calculations of electrostatic effects with continuum methods, it will be necessary to learn to account quantitatively for the contributions by solvent penetration to dielectric effects in the protein interior.

INTRODUCTION

The development of computational tools for the efficient and accurate estimation of electrostatic energies from structure continues to attract considerable interest. Calculations of electrostatic contributions to energetics are important in problems of stability, macromolecular recognition, and design of proteins. There are also innumerable examples where they are essential for understanding functional energetics in structural terms. Many of the computational problems that had to be addressed to make these calculations possible, such as the calculation of electrostatic potentials in the protein–solvent system, and the rigorous treatment of cooperative proton binding in multi-site systems, have been solved (Matthew et al., 1985; Sharp and Honig, 1990; Warshel and Åqvist, 1991). The quantitative treatment of dielectric effects in the protein interior is the main remaining problem that currently limits the accuracy, reliability, and utility of structure-based calculations of electrostatic energies with continuum approaches.

The surface of a protein represents an interface between substances of very different dielectric properties. In energy calculations with microscopic methods, these properties can be captured, at least in principle, through the explicit treatment of electronic polarizability and of dipolar relaxation of both protein and solvent. In calculations with semimicroscopic or with continuum methods the dielectric properties of the protein interior and of the solvent phase are represented in terms of dielectric constants. The concept of the dielectric constant is not necessarily compatible with the size, complexity, and heterogeneity of the protein interior. Furthermore, it is not clear that use of a single dielectric constant to represent permittivity in an environment that is inherently anisotropic is valid. Nevertheless, continuum methods remain extremely popular due to their promise of fast, efficient, and potentially reliable energy calculations.

A dielectric constant of 4 is commonly used in continuum methods to model the dielectric properties of the protein interior. This is also the value of the dielectric constants of crystalline and polymeric amides (Gregg, 1976), and of dry protein and peptide powders (Bone and Pethig, 1982, 1985; Harvey and Hoekstra, 1972). Similar dielectric constants are predicted for proteins by a variety of theoretical calculations based on normal mode analysis and on molecular dynamics simulations (Gilson and Honig, 1986; Löffler et al., 1997; Simonson and Perahia, 1995; Smith et al., 1993).

A dielectric constant of 4 is much lower than the dielectric constant of water (78.5 at 25°C), but it represents substantial polarizability relative to vacuum. Nevertheless, the magnitude of electrostatic energies in proteins is grossly exaggerated in continuum calculations with static structures when a low dielectric constant is used. This problem is most acute in calculations involving groups buried within the protein interior. Paradoxically, the polarizability experienced by these groups is considerably higher than the polarizability corresponding to a dielectric constant of 4 (García-Moreno et al., 1997 and references therein). Physical mechanisms must be at play that contribute to the polarizability in the interior of proteins in ways that are not evident in crystallographic structures, nor represented by the static

Received for publication 14 March 2000 and in final form 7 June 2000.

Address reprint requests to Bertrand García-Moreno E., Department of Biophysics, Johns Hopkins University, 3400 N. Charles St., Baltimore, MD 21218. Tel.: 410-516-4497; Fax: 410-516-4118; E-mail: bertrand@jhu.edu.

Dr. Dwyer's present address is Trimeris Inc., Department of Biophysical Chemistry, 4727 University Drive, Durham, NC 27707

0006-3495/00/09/1610/11 $2.00

dielectric constant of dry proteins, nor captured by theoretical estimates of the protein dielectric constant. Several molecular mechanisms have been proposed previously to rationalize the apparent high polarizability inside proteins: reaction field of bulk solvent (King et al., 1991; Löffler et al., 1997), solvation by permanent dipoles in the protein (Warshel et al., 1989), conformational relaxation (Antosiewicz et al., 1994), fluctuations of surface charged side chains (Simonson and Brooks, 1996; Simonson and Perahia, 1995; Smith et al., 1993), and transient exposure to solvent by penetration or by local or global unfolding (Warshel et al., 1984). None of these conjectured mechanisms have been corroborated experimentally.

Empirical approaches have been devised in efforts to attenuate artificially the electrostatic energies estimated in proteins with continuum methods. Some involve the use of parameters based on solvent accessibility (Matthew et al., 1985), or the ad hoc use of arbitrarily high protein dielectric constants (Antosiewicz et al., 1994). The same effect can be achieved by incorporation of explicit water molecules in the calculations (Gibas and Subramanian, 1996). In the most physically appealing calculations, the protein interior is treated with a low dielectric constant (2 to 4) and the realistic magnitude of electrostatic energies is achieved through the explicit treatment of conformational flexibility (Havranek and Harbury, 1999, and references therein). These empirical modifications markedly improve the ability of continuum algorithms to capture correctly the ionization behavior of surface groups. However, they are less successful at improving estimates of electrostatic interaction energies in or through the protein interior. This remains problematic. Unfortunately, these are the cases that matter the most. It is in the interior of proteins, or at buried locations in the interfaces between proteins, where recognition, catalysis, REDOX reactions, photoactivation, H^+ and e^- conduction, and other key biological phenomena that are governed by electrostatics take place.

Progress in overcoming the problem of the dielectric properties of proteins has been hindered by the lack of experimental systems where the structural and physical origins of dielectric effects could be elucidated, and with which models and theoretical predictions could be tested quantitatively and calibrated. Toward this end, we have initiated systematic structural and thermodynamic studies of proteins in which ionizable groups have been artificially introduced into the hydrophobic core by site-directed mutagenesis (García-Moreno et al., 1997; Stites et al., 1991). Here, we present crystallographic structures and stability measurements of a mutant of staphylococcal nuclease termed PHS/V66E, in which a Glu has been buried in the hydrophobic core by replacement of Val-66. PHS nuclease, a hyperstable form of the protein, was used in these experiments to maximize the pH range where the protein remains folded after ionization of the buried Glu-66. The pK_a value of the buried Glu was determined by two completely independent equilibrium thermodynamic methods: indirectly, by analysis of the pH dependence of stability of mutant and wild type protein with linkage relationships, and directly, from the difference in proton titration curves measured potentiometrically in background and mutant proteins. Crystallographic structures were determined under conditions of pH where the buried Glu is neutral. Similarities and some remarkable differences were observed between the behavior and the milieu of the buried side chains of Glu-66 and Lys-66.

Buried acidic residues, like the one introduced artificially in PHS/V66E, have been identified as the essential functional motifs in membrane proteins involved in proton conduction (Deisenhofer and Michel, 1989; Ermler et al., 1994; Luecke et al., 1998; Martinez et al., 1996; Pebay-Peyroula et al., 1997). Insights from the correlation of structure and energy of the Glu-66 mutant will deepen our understanding of these interesting biological systems at the molecular level.

MATERIALS AND METHODS

Protein engineering

The V66E mutation was introduced into the hyperstable form of nuclease known as PHS, originally engineered by Prof. David Shortle at Johns Hopkins University School of Medicine. PHS involves mutations P117G, H124L, and S128A. PHS and PHS/V66E nuclease were expressed and purified following the method of Shortle and Meeker (1986). The protein was determined to be >98% pure by SDS-PAGE. The concentration was determined using a value of 0.93 for the absorbance of a 1 mg/ml sample at 280 nm.

Potentiometric proton titration curves

The experimental procedure for the measurement of proton binding curves by direct potentiometric methods has been presented previously (García-Moreno et al., 1997). Proton titration curves of PHS and PHS/V66E nuclease were measured from pH 5.0 to 10.0 with 3 ml of 1.0–1.2 mg/ml protein solution in 0.1 M KCl. Titrant consisted of calibrated 0.02 N NaOH or HCl. It was dosed in 5-μl increments. All titration curves were measured in triplicate. Reversibility of the titration curve was routinely tested. Titration curves were fitted with eighth-order polynomials. The difference between the two proton titration curves represents the titration of Glu-66 and of all other groups whose pK_a values are perturbed by the Val→Glu mutation. The pK_a of Glu-66 in the native state was obtained by nonlinear least squares fit of the difference titration curve with the modified Hill equation,

$$\Delta\nu_i = \frac{10^{n(pH-pK_a)}}{1 + 10^{n(pH-pK_a)}}. \quad (1)$$

Analysis of the difference proton titration curve with Eq. 1 assumes that the Val→Glu mutation at position 66 does not significantly affect the ionization properties of other titratable groups.

Equilibrium denaturation

The pK_a of Glu-66 was also obtained from the difference in denaturational free energies of PHS and PHS/V66E proteins measured by guanidine

hydrochloride (GdnHCl) denaturation over a wide range of pH values. All measurements were performed with the ATF-105 automated titration differential spectrofluorometer by Aviv (Lakewood, NJ). GdnHCl denaturation was performed with protein concentration of 50 μg/ml at 25°C in 100 mM NaCl plus 25 mM buffer. Acetate was used in the pH range from 4 to 5.5, MES from 5.5 to 6.5, HEPES from 7 to 8, TAPS from 8 to 9, CHES from 9 to 10, and CAPS from 10 to 11. The fluorescence of the single tryptophan at position 140 was used to monitor denaturation, as described previously (Stites et al., 1991; 1995). Equilibration times between addition of denaturant were longer for PHS nuclease and its mutants than for the wild type protein. Denaturational transitions were analyzed assuming a two-state model for reversible denaturation.

The pK_a of Glu-66 in the native and in the unfolded states was obtained by fitting the difference between the pH-dependent stability of the background and mutant proteins ($\Delta\Delta G^o_{H_2O}$) with

$$\Delta\Delta G^o_{H_2O}(pH) = \Delta\Delta G^o_{H_2O}(mut) - RT \ln \frac{1 + e^{2.303\,(pK_a^D - pH)}}{1 + e^{2.303\,(pK_a^N - pH)}}. \quad (2)$$

The properties and limitations of this function have been discussed previously (Stites et al., 1991). In this expression, pK_a^N and pK_a^D refer to the pK_a of Glu-66 in the native and in the denatured states, respectively. The pH-dependent contributions to $\Delta\Delta G^o_{H_2O}$ are captured by the right-most term. The pH-independent component ($\Delta\Delta G^o_{H_2O}(mut)$) reflects the energetic consequences of the mutation independent of the electrostatic effects associated with shifts in pK_a. This function assumes that the pH dependence of $\Delta\Delta G^o_{H_2O}$ is determined solely by the pK_a of Glu-66. Specifically, it assumes that the mutation does not significantly affect the ionization properties of other titratable groups. The validity of this assumption has been discussed previously (García-Moreno et al., 1997).

Acid and base denaturation of PHS and PHS/V66E monitored by fluorescence was performed as described previously (García-Moreno et al., 1997; Stites et al., 1991). All measurements were performed with the Aviv ATF-105 automated titration fluorometer. The experiments were performed with a protein concentration of 50 μg/ml, at 25°C in 100 mM NaCl plus 25 mM buffer.

X-ray crystallography

PHS/V66E nuclease was crystallized using the vapor diffusion method at pH 8.0 in 59–61% (vol/vol) 2-methyl-2,4-pentanediol and 10.5 mM KPO_4 buffer using a protein concentration of 12.2 mg/ml. Crystals were also obtained at pH 6.0 in 60–61% (vol/vol) MPD in 10.5 mM KPO_4 with protein concentration of 16 mg/ml. Crystals at pH 8 appeared in 1–2 weeks at 4°C. Data were collected with a single crystal using an R-AXIS IIc image plate detector (Rigaku, Danvers, MA). The crystal was placed in a thin loop, with the crystallization buffer as a cryosolvent, and flash frozen under a steady stream of nitrogen at −178°C. Crystals were found to be isomorphous to those of the uncomplexed, wild type nuclease, and this structure (1stn in Protein Data Bank) was used as an initial model. The glutamic acid at position 66 as well as the H124L and S128A mutations in PHS nuclease were initially modeled as glycine to avoid biasing the side chain conformation. Refinement was carried out using the program XPLOR (Brünger et al., 1987; Brünger, 1992) over the resolution range 6.5–2.1 Å, to a final R value of 18.64, and R_{free} of 26.6%. The side chain of the glutamic acid, and the other point mutations, were built into the calculated 2Fo-Fc and Fo-Fc electron density maps with the program CHAIN (Sack, 1988, 1993). Electron density that was modeled as four water molecules was present near the side chain of position 66 in the structures at pH 6 and 8, in both 2Fo-Fc and Fo-Fc maps, contoured at 1σ and 3.5 σ, respectively. The water molecules were prominent in the first cycle of refinement. Omit 2Fo-Fc, and Fo-Fc maps of the electron density were calculated after refinement with the four water molecules excluded. Very strong density was observed at the position of the four omitted water molecules in both maps (contoured at 1σ and 3.5 σ cutoff), confirming the presence of the water molecules. B factors of the water molecules were comparable to those of the surrounding backbone atoms. Coordinates are available through the Protein Data Bank.

RESULTS

Acid/base denaturation and pH dependence of stability

The acid/base titrations of PHS and PHS/V66E monitored by fluorescence are shown in Fig. 1. Because of its higher intrinsic stability, PHS acid denatured at a pH a full unit below the midpoint of the acid denaturation of the wild type staphylococcal nuclease (data for wild type not shown). PHS/V66E acid unfolds at higher pH values because of the loss of stability stemming from the replacement of Val-66 by Glu.

As expected, the base denaturation of PHS/V66E was shifted toward more acidic pH values. This reflects primarily the loss of stability related to the shift in pK_a of Glu-66 as a result of its burial in the hydrophobic core. The base denaturation of PHS nuclease was not as cooperative as its acid denaturation. To rule out the possibility that this reflected changes in the protonation state of the Trp fluorophore, we established that the fluorescence of the Trp analog NATA (*N*-acetyl tryptophan amide) is pH independent in the pH range explored in Fig. 1 (data not shown). There are seven tyrosines in staphylococcal nuclease, and, in this pH range, tyrosinate in water can fluoresce, possibly con-

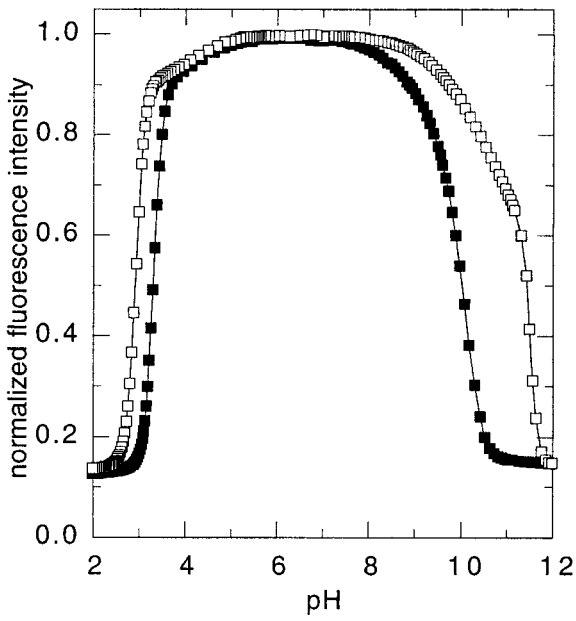

FIGURE 1 Acid/base titration of PHS (*open squares*) and PHS/V66E (*solid squares*) in 100 mM NaCl at 25°C monitored by fluorescence. The lines through the data are for visual reference only.

tributing to the complex shape of the base titration of PHS nuclease monitored by fluorescence.

The pH dependence of stability of PHS and PHS/V66E nuclease measured by GdnHCl denaturation is shown in Fig. 2. The stability of PHS was almost pH independent over the broad range of pH between 10 and 5. It begins to decrease at pH 5 because of the depressed pK_a values of Glu and Asp residues in the native state relative to their pK_a values in the denatured state (Whitten, 1999). At the other end of the pH scale, the stability of PHS began to decrease markedly at pH 9.5. According to GdnHCl denaturation, the stability of PHS is significant even at pH 11, whereas, according to the titration monitored by fluorescence, half of the molecules are unfolded at this pH. This further suggests that the shoulder in the base titration of PHS monitored by fluorescence originates with chromophores other than Trp-140, and does not report the unfolding of the protein with great fidelity.

The pH dependence of stability of PHS and PHS/V66E are very different. At pH values below the normal pK_a of 4.5 of a Glu in solution, the difference in stability between PHS and PHS/V66E is approximately 3 kcal/mol. This represents the penalty for replacing Val-66 with a neutral Glu-66. At pH values above the normal pK_a of Glu in water, the stability of PHS/V66E decreases by approximately 1.1 kcal/mol per pH unit. This is very close to the theoretical loss of 1.36 kcal/mol of stability per pH unit that would be predicted at 25°C based on the difference between the normal pK_a of Glu in water and the pK_a of the buried Glu-66. The pH dependence of stability of PHS/V66E is dominated by the loss of solvation of the buried Glu. The pK_a values of most other ionizable groups in the protein appear not to be greatly affected by the Val→Glu mutation. In the difference free energy curve shown in Fig. 2, the decrease in stability with increasing pH levels off at approximately 9.5. Therefore, the buried Glu must ionize with a pK_a value below 9.5. The stability of the PHS/V66E protein reached a value of 0 very close to pH 10, consistent with the midpoint of the base titration monitored by fluorescence. At this pH, half of the protein molecules are still folded.

Proton binding measurements

The proton titration curves of PHS and PHS/V66E, and the difference between these two curves, are shown in Fig. 3. The proton binding properties of the two proteins are almost identical below pH 8. At pH values above 8, more protons were released by PHS/V66E than by PHS. The fit of a single-site Langmuir isotherm to the difference curve between pH 7.5 and 9 was excellent. The substantial proton release by PHS/V66E at pH values above 9 signals the onset of base denaturation. It is consistent with the conformational transition that is reflected in the base titration monitored by fluorescence.

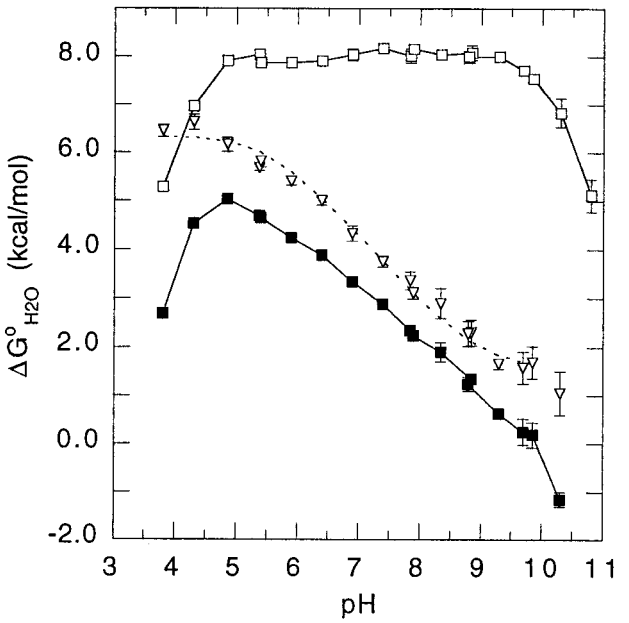

FIGURE 2 pH dependence of stability ($\Delta G^{o}_{H_2O}$) measured by GdnHCl denaturation for PHS (*open squares*) and PHS/V66E (*solid squares*) at 25°C in 100 mM NaCl. Open triangles represent the difference in stability between these two proteins, shifted arbitrarily along the ordinate. The dotted line through the difference curve was obtained by fitting with Eq. 2.

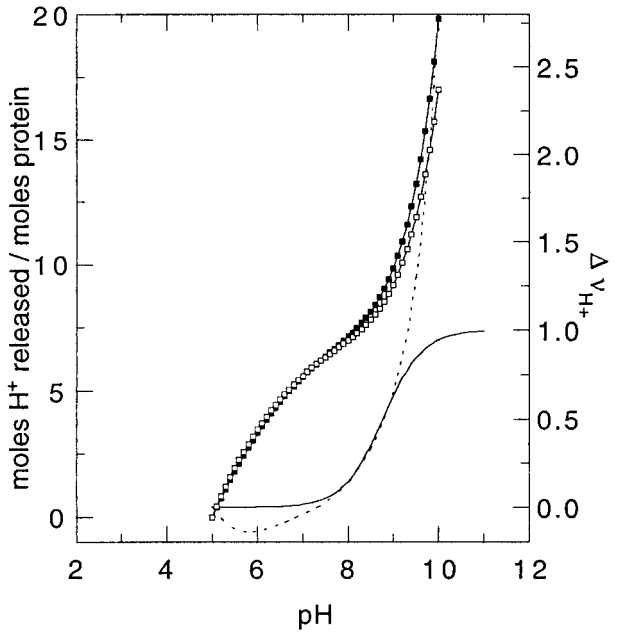

FIGURE 3 Proton titration of PHS (*open squares*) and PHS/V66E (*solid squares*) measured potentiometrically at 25°C in 100 mM KCl. The lines and the points are fits of the raw data with eighth-order polynomial. The dotted line represents the difference of the polynomial fits to the proton binding curve (PHS/V66E − PHS), plotted with reference to the right axis. Superimposed on the dotted line is the single site proton binding isotherm for a group with pK_a of 8.8.

The proton titration curves measured potentiometrically, the acid/base titration monitored by fluorescence, and the chemical denaturation studies indicate that, although PHS/V66E is highly destabilized under conditions of pH where the buried Glu-66 is ionized, it still exists mostly as a folded protein. More than 70% of the protein molecules remain folded at pH 9.8, where 90% of the buried Glu residues are ionized. The Δ+PHS/V66K mutants of nuclease (García-Moreno et al., 1997; Stites et al., 1991) and the M102K mutant of T4 lysozyme (Dao-Pin et al., 1991) are other examples of proteins that remain folded and presumably in native-like states after ionization of a group artificially buried in the hydrophobic core.

pK_a of the buried Glu-66

Robust measurements of pK_a values are essential for the interpretation of ΔpK_a values in terms of apparent dielectric constants. This is why the pK_a of Glu-66 was measured by two completely independent equilibrium experiments. The agreement between pK_a values obtained by the two different methods was excellent. The value measured by analysis of the difference proton binding curves was 8.8 (Fig. 3). A pK_a of 8.5 was obtained by analysis of the stability curves (Fig. 2) when the pK_a of Glu-66 in the denatured state was fixed at 4.5, the value measured previously for Glu in the Gly-Glu-Gly peptide in solution (Matthew et al., 1985). When, instead, the pK_a of Glu-66 in the denatured state was allowed to float, a pK_a of 9.0 was obtained for Glu-66 in the native state. The shift in pK_a from 4.5 to 8.8 amounts to a Gibbs free energy difference of 5.8 kcal/mol. The pK_a shifts of Glu-66 and Lys-66 are almost identical. This suggests that these groups are in environments of very similar net polarizability.

The analysis of thermodynamic data with Eqs. 1 and 2 to obtain the pK_a of Glu-66 assumes that the ionization properties of other ionizable groups are not perturbed by the Val→Glu mutation at position 66. Previously, we tested the validity of this assumption by demonstrating that the pK_a value of an individual histidine obtained from this type of thermodynamic analysis was identical to the value measured directly with NMR (García-Moreno et al., 1997). In the specific case of PHS/V66E, the data in Figs. 2 and 3 validate this assumption. The overlap in the proton titration curves of background and mutant protein between pH 5 and 8 in Fig. 2 demonstrates that the pK_a of other ionizable groups that titrate in this range of pH are not significantly altered by the mutation. The difference potentiometric titration curve is dominated by the large proton release associated with the titration of the buried Glu-66. Similarly, the excellent fit of the $\Delta\Delta G^{o}_{H_2O}$ versus pH curve (Fig. 3) with Eq. 2, and the sign and magnitude of the slope of the pH dependence of $\Delta G^{o}_{H_2O}$ for PHS/V66E demonstrate that the pK_a shift of the buried Glu-66 is responsible for the pH dependence of $\Delta\Delta G^{o}_{H_2O}$.

Crystallographic structures of PHS/V66E

In the crystallographic structures of V66K mutants of nuclease published previously (García-Moreno et al., 1997; Stites et al., 1991) the side chain of Lys-66 in the neutral state is buried in a completely hydrophobic environment inside the β barrel of the protein (Fig. 4 *A*). Those structures did not reveal any clues about the plausible physical or structural origins of the high polarizability experienced by ionizable residues buried at this location. The structures are

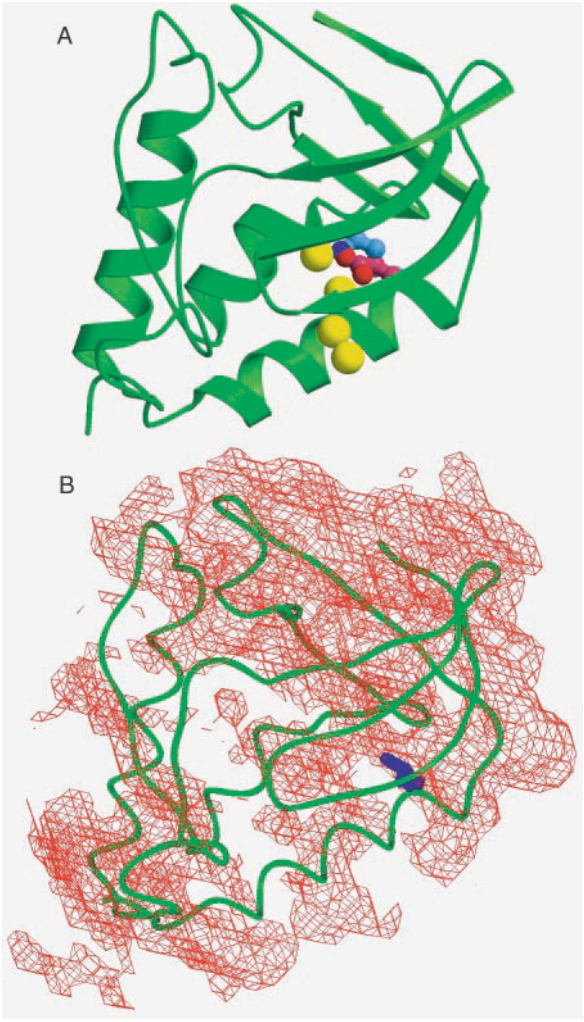

FIGURE 4 (*A*) Structure of PHS/V66E nuclease. The buried side chain of Glu-66 is shown in red. The buried side chain of Lys-66, shown in blue, is superimposed for comparison. The water molecules that penetrate into the core of the structure are represented as yellow spheres. This image was drawn with MOLSCRIPT and RASTER 3D (Kraulis; 1991; Merrit and Bacon, 1997). (*B*) Packing density of wild type nuclease oriented as in panel *A*. The side chain at position 66 is shown in blue. The packing density was calculated with the method of Privalov (1995) with the MOLE molecular graphics software package (Applied Thermodynamics Inc.). The packing density cutoff was set arbitrarily high to show that the pathway of the chain of waters coincides with a channel of very low packing density. The void represents areas where the packing density is below the cutoff value.

superimposable with those of wild type nuclease. In the high resolution crystallographic structures of PHS/V66E nuclease at pH 6 and 8, the neutral Glu-66 side chain is buried in almost the exact same environment and orientation as the buried Lys-66 side chain (Fig. 4 *A*). The OE1 and OE2 atoms of Glu-66 are approximately 10.9 and 9.5 Å away from bulk solvent. The only polar atom near the Glu-66 side chain is the hydroxyl oxygen of Thr-62, which is 3.13 Å away from the nearest carboxyl oxygen. All atoms in van der Waals contact with the oxygen atoms in the carboxyl moiety are nonpolar. The charged side chain nearest to Glu-66 is Asp-19, which is solvent exposed and 8.1 Å away.

The most remarkable feature of the PHS/V66E structure is a chain of 4 water molecules that was found connecting the buried, uncharged side chain of Glu-66 with bulk solvent (Figs. 4 *A* and 5). The temperature factors of this region of the protein are low and the water molecules appear to have a high degree of positional order. The two outermost water molecules (W3 and W4 in Fig. 5) have been seen previously; W3 in all but two of the 18 deposited crystallographic structures of nuclease and its mutants, W4 in approximately half of them. The two innermost water molecules (W1 and W2 in Fig. 5) have never been seen previously, not even in mutants with Lys, Ala, Gly, or Ile at position 66, nor in structures of nuclease in which the hydrophobic core has been disrupted by mutations elsewhere. The structure of PHS/V66E nuclease is superimposable on the more than twenty crystallographic structures of nuclease and its mutants (r.m.s. between PHS/V66E and Δ+PHS/V66K, for example, is only 0.32 Å). The water molecules that penetrate into the hydrophobic core are accommodated and ordered without any apparent disruptions in packing or in hydrogen bonding patterns in this region of the protein. The area of the protein where the water molecules were found coincides with one of the regions of lowest packing density in the structure (Fig. 4 *B*).

In a statistical survey of crystallographic structures, buried water molecules were found most frequently at buried turns between consecutive strands in β sheets (Rose et al., 1983). At these locations, the buried water molecules satisfy the hydrogen bonds that cannot be made internally by the backbone polar atoms at the turn. Although the chain of water molecules in PHS/V66E is, in fact, nestled between helix 1 and the buried reverse turn between β strands 1 and 2, consisting of residues 19 through 22, the backbone dipoles of residues 20 and 21 do not interact directly with waters W1 and W2. The carbonyl oxygen at position 22 is hydrogen bonded to water molecules W1 and W2. The other hydrogen bonds in this region of the protein are identical in the structures of wild type nuclease and its mutants, including PHS/V66E (Fig. 5).

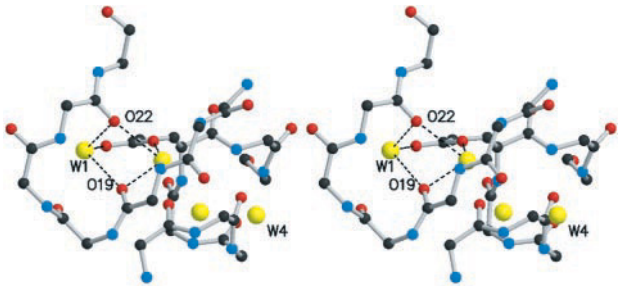

FIGURE 5 Stereo view showing the interactions between the four water molecules, the buried side chain of Glu-66, and the backbone atoms of residues 19–22 in strands 1 and 2 of the β barrel. The dotted lines outline the two puckered pentagonal structures that are made by the two carboxylic oxygen atoms, the two water molecules, and the backbone oxygen atoms at positions 19 and 22. Image drawn with MOLSCRIPT and RASTER 3D (Kraulis, 1991; Merrit and Bacon, 1997).

Interpretation of ΔpK_a in terms of apparent dielectric constants

A quantitative understanding of the molecular origins of pK_a values of buried ionizable groups requires microscopic calculations where all interactions are treated explicitly and without assumptions about dielectric constants. Such calculations are beyond the scope of this report. A detailed study involving calculations with semimicroscopic and with continuum electrostatic methods is underway and will be presented elsewhere.

A reverse pK_a calculation is one of the ways in which the apparent dielectric constants (D_{app}) in the protein interior can be estimated from pK_a values of buried groups obtained experimentally. This is a strictly model-dependent approach: the apparent dielectric constants thus obtained depend on the way in which they are defined and on the model used to obtained them (Churg and Warshel, 1986; Warshel and Åqvist, 1991; Warshel et al., 1997; references therein). In the case of Lys-66, the D_{app} value that was obtained by analysis of the pK_a shift with a simple Born formalism (García-Moreno et al., 1997) is nearly identical to the one obtained with more rigorous and sophisticated inverse pK_a calculations based on the numerical solution of the Poisson Boltzmann electrostatics by finite differences (Antosiewicz et al., 1994). This implies that the shift in the pK_a of the buried Lys-66 was determined primarily by the energetics of desolvation, with only minimal contributions by interactions with surface ionizable groups or other polar atoms.

The D_{app} value represented by the difference in pK_a between Glu-66 and a solvent exposed Glu (pK_{ref}) was calculated with the Born formalism,

$$1.36z(pK_{ref} - pK_a) = \frac{332Z^2}{2r_{cav}}\left(\frac{1}{D_{app}} - \frac{1}{D_{H_2O}e^{\kappa^* r_{cav}}}\right) + \frac{332Z^2}{2r_{prot}}\left(\frac{1}{D_{H_2O}e^{\kappa r_{prot}}} - \frac{1}{D_{app}}\right). \quad (3)$$

This function describes the Gibbs free energy (kcal/mol) for transferring an ion of valence Z and cavity radius r_{cav} (Å) from water into the center of a low dielectric sphere of radius r_{prot} (Å) that is surrounded by water. This function reduces to the original Born expression for the solvation free energy of ions when r_{prot} is large.

A D_{app} value of 9.5 was estimated when values of r_{cav} of 2.17 Å and r_{prot} of 12 Å were assumed in the analysis of the ΔpK_a of 4.3 measured for Glu-66. The D_{app} obtained for the buried Lys-66 with these same parameters and with Eq. 3 is 9.0. To estimate how D_{app} values would be affected by uncertainties in the parameters in Eq. 3, the variation in D_{app} with r_{cav}, r_{prot} and ΔpK_a was mapped explicitly. Errors of ± 0.30 in ΔpK_a translate to $\sim \pm 0.50$ in D_{app}. An increase of 0.67 Å in r_{cav} would decrease D_{app} to 7, and a decrease in r_{cav} by the same amount would increase D_{app} to 13.8. D_{app} is least sensitive to r_{prot}: changes of 2.0 Å translate to changes in D_{app} of 0.3. When the rightmost term in Eq. 3 is ignored, the D_{app} reported by Glu-66 is 11.5 and by Lys-66 it is 11. This suggests that the high dielectric medium surrounding the protein does not make a significant contribution to D_{app} at these sites because they are buried too deeply in the hydrophobic core of the protein.

DISCUSSION

The shifts in pK_a experienced by Glu and Lys residues when buried at position 66 in staphylococcal nuclease are consistent with a net polarizability in the protein interior considerably higher than the polarizability reflected in the static dielectric constants of 2 to 4 measured in dry proteins and peptides. The structure of the V66K mutants of staphylococcal nuclease did not offer any insights about the structural origins of the high apparent polarizability in the core of this protein. The neutral Lys side chain was found nearly 12 Å from the bulk solvent, entirely surrounded by nonpolar atoms, without polar atoms within van der Waals contact, far from other ionizable groups. The surprising finding in the structures of PHS/V66E nuclease was the presence of a string of water molecules that hydrate the neutral and buried Glu-66 side chain, and connect it with bulk solvent. These structures suggest that the high D_{app} in the interior of staphylococcal nuclease reflects the presence of water molecules that penetrate into the hydrophobic core of the protein. The similarities in the pK_a shifts measured for Glu-66 and for Lys-66 imply that the polar moieties of the buried Lys and Glu side chains experience environments of equivalent net polarizability. With the data at hand, it is not possible to exclude the possibility that the high polarizability experienced by Lys-66 originates from dipolar rotation in the protein matrix. However, the presence of buried water molecules in the structures of the V66E mutant, and the similarity in the ΔpK_a experienced by the buried Lys and Glu residues, suggests that the high polarizability experienced by Lys-66 also reflects hydration by transient solvent penetration or by disordered buried water molecules that are not visible crystallographically.

One of the structural reasons why the buried Glu side chain is hydrated is that the side chain is accommodated in a small cavity where there is room for solvent. The cavity that is occupied by W1 and W2 has an elongated, pore-like shape instead of the globular shape typical of cavities in monomeric proteins (Williams et al., 1994). Because of this elongated shape, the volume of the cavity was very small when it was measured with the standard 1.4-Å probe. With a 1-Å probe, its volume was estimated to be 8.0 $Å^3$, enough to accommodate two tightly packed water molecules. When the waters are bound there is no open space in the cavity.

Unlike the buried water molecules characterized in other proteins by NMR, which have been described as being merely trapped and not interacting strongly with the protein (Denisov et al., 1996), the water molecules that are visible in diffraction experiments are those that are positionally ordered (i.e., they spend a significant fraction of time in given positions) because they are tethered to polar and ionizable groups directly or through a network (Sreenivasan and Axelsen, 1992). Waters W1 and W2 in PHS/V66E are positionally ordered because several factors act synergistically to define minima at the water positions on the potential energy surfaces. The intrinsic hydrogen-bonding potential of the Glu side chain is high (Roe and Teeter, 1993; Thanki et al., 1988; Wimley et al., 1996). In addition, waters W1 and W2 occupy positions relative to OE1 and OE2 that correspond to the statistically most favored positions for hydration of Glu and Asp side chains (Roe and Teeter, 1993; Thanki et al., 1988). Furthermore, the set of atoms consisting of W1, W2, the backbone carbonyl oxygen atoms of residues 19 and 22, and the OE1 and OE2 atoms of Glu-66 are in the slightly puckered pentagonal arrangements typical of waters ordered by proteins (Teeter, 1984) (Fig. 5). These pentagonal structures optimize the O–O–O angles at tetrahedral values, and, for this reason, are thought to be one of two preferred structures in liquid water (Liu et al., 1996).

It is not surprising that water molecules W1 and W2 are positionally disordered and crystallographically invisible in the absence of the buried Glu-66 side chain. In wild type nuclease, the cavity is larger than in the V66K or V66E mutants because the volume of the Val side chain is smaller than the volume of Lys or Glu side chains. More than two water molecules could easily fit in the cavity in the wild type protein. However, in the wild type structure, the cavity is lined with apolar atoms everywhere except at the buried β turn involving residues 19 to 22. The absence of strong preferential binding sites precludes the positional ordering of waters in the cavity, rendering them invisible in the diffraction experiment. If the waters are present but disordered in the wild type protein, they might be visible by NMR, which detects waters based on their lifetimes.

It is less obvious why the water molecules are not seen crystallographically in the mutants with Lys-66. The ionization energetics of Lys-66 suggests that, at least in the charged state, but probably also in the neutral state, the buried Lys side chain is in contact with water. This contact could arise from transient penetration, or from interactions with buried waters that are disordered and not visible crystallographically. There are several structural reasons why water molecules W1 and W2, which were positionally ordered in the structure of the V66E mutant, might be present but disordered in the V66K mutant. The intrinsic hydrogen-bonding potential of the Lys side chain is lower than that of the Glu side chain (Thanki et al., 1988); in general, carboxyl groups are better hydrated than amines (Collins, 1997). In the structures of mutants with Lys-66, the volume of the cavity is only 5.4 $Å^3$, nearly 33% smaller than the volume of the cavity when position 66 is a Glu. On the one hand, the smaller volume of this cavity should have an ordering effect on the waters, and on the other hand, the volume of the cavity might not be large enough to accommodate W1 and W2 simultaneously in stable bound positions. The observed preference of water for the buried Glu over the buried Lys side chain is entirely consistent with the acknowledged role of Glu, Gln, Asp, Asn, Tyr, Ser, and Thr as the preferred side chains for stabilizing buried water molecules in other proteins (Buckle et al., 1996; Deisenhofer and Michel, 1989; Ermler et al., 1994; Luecke et al., 1998; Martinez et al., 1986; Meyer, 1992; Ormö et al., 1996; Otting et al., 1991; Pebay-Peyroula et al., 1997; Shih et al., 1995; Sreenivasan and Axelsen, 1992).

The hypothesis that solvent penetration can contribute substantially to the high polarizability inside a protein is consistent with the recognized ability of water (Ernst et al., 1995; García and Hummer, 2000; Oprea et al., 1997; Otting et al., 1997; Tüchsen et al., 1987, Woodward et al., 1982) and other small molecules (Feher et al., 1996) to diffuse inside proteins rapidly and with small activation barriers. It is also supported by the increasing number of crystallographic structures where buried ionizable groups, especially acidic ones, are found in a hydrated state (Dao-Pin et al., 1991; Ermler et al., 1994; Martinez et al., 1996; Meyer, 1992; Ormö et al., 1996; Pebay-Peyroula, 1997; Roe and Teeter, 1993; Shih et al., 1995; Sreenivasan and Axelsen, 1992). In the specific case of the core of staphylococcal nuclease, three different factors favor hydration of the buried side chain at position 66: 1) there is a small cavity in the region where waters can be accommodated without disruption of the rest of the structure, 2) the packing density in the channel occupied by the water molecules is low, and 3) one of the walls of the cavity consists of a buried β turn, which buries two backbone carbonyls that are not hydrogen bonded within the protein. To test the generality of the hypothesis that the high apparent polarizability in the interior of proteins reflects solvent penetration, we have initiated studies of the energetics of ionization of residues buried at other sites in staphylococcal nuclease and in other proteins.

It has been demonstrated by NMR that the buried water molecules that are seen crystallographically in BPTI have residence times between 10^{-6} and 10^{-4} sec if deeply buried, and 10^{-8} to 10^{-6} sec if closer to the surface (Denisov et al., 1995). The fast exchange is probably limited only by the small structural fluctuations required for passage of individual water molecules in and out of the interior of the protein. By visual inspection of the crystallographic structures, the environments of the buried water molecules in nuclease and in BPTI appear to be similar. If the dynamics relevant to solvent penetration and exchange are comparable between these two proteins, the exchange rates of buried solvent should be equally fast. Interactions between fast exchanging water molecules and the buried ionizable groups, averaged over the slow time scale of the equilibrium experiments used to measure pK_a values, could result in high D_{app} values. The observation that the equilibrium dielectric constant of liquid water is 80 even at frequencies as high as 10 GHz (Pethig, 1979) suggests that D_{app} could arise from interactions between buried ionizable groups and buried but disordered waters, or with transiently buried water molecules, even if their exchange is as fast as the fastest that has been measured by NMR.

In a medium of low dielectric constant, charges can be solvated very effectively by a few water molecules or by other sources of permanent dipoles (Gibas and Subramanian, 1996; Warshel and Åqvist, 1991; Warshel et al., 1997). If the true dielectric constant of the protein substance is low, the buried water molecules can contribute significantly to the apparent polarizability reported by the measured pK_a values. The following calculation affords a simple semiquantitative estimate of the magnitude of the effect of buried water molecules on the pK_a of Glu-66. Assuming a value of 4 for the dielectric constant inside a protein (Bone and Pethig, 1982, 1985; Harvey and Hoekstra, 1972), then the expected pK_a difference between Glu in water and Glu in the core of the protein according to a Born formalism would be $\approx$18–25 kcal/mol, depending on the size of the cavity radius used in the calculation with Eq. 3. The effect that a single buried water dipole could have on the pK_a in this dielectric environment can be estimated from the energy of interaction between the water dipole and the charged form of the buried ionizable group calculated with

$$\Delta G_{\text{charge-dipole}}\ (\text{kcal/mol}) = \frac{(-69.11 Z\mu \cos\theta)}{(Dr^2)}. \qquad (4)$$

In this expression, μ is the dipole moment of water (1.84 Debye), Z is the net charge on the ionized carboxylic side chain, r is the distance (Å) between the center of the dipole and the carboxyl oxygen, and θ describes the orientation of the dipole. Assuming that the water dipole is aligned perfectly with the field of the charge ($\theta = 180°$), that r is 2 Å,

and that D is 4, then the calculated $\Delta G_{\text{charge-dipole}}$ is -7.9 kcal/mol per water molecule. Interactions between the buried group and a pair of water molecules could easily account for the modest shift in pK_a that are measured, relative to the ones that are predicted when the protein interior is treated as a medium of low dielectric constant, and when the presence of the buried water molecules is ignored.

A particularly dramatic example of the efficacy with which buried ionizable groups can be solvated by buried water is the ΔpK_a of only 1.2 units that was measured for a buried Asp in chicken egg white lysozyme (Shih et al., 1995). The higher apparent polarizability experienced by this buried Asp correlates with the presence of four conserved, internal water molecules in contact with the Asp side chain. The solvation of the buried side chain by these four buried waters is almost as effective as in bulk water. A recent report of the depressed pK_a of the buried Asp-76 in ribonuclease T1, which is surrounded by water molecules and permanent dipoles of the protein, demonstrates that the protein matrix itself can solvate buried charged groups very effectively, even more effectively than water itself (Giletto and Pace, 1999). According to Warshel and colleagues (1978, 1989), this is likely to be the case in naturally occurring buried ionizable groups, where the protein matrix can evolve to fine tune solvation of buried groups.

Many mechanisms have been proposed by others to rationalize the discrepancy between the static dielectric constants measured with classical methods in dry protein powders and peptides, and the high apparent polarizability in the interior of globular proteins in solution obtained by analysis of ionization energetics of single or ion-paired buried groups. The structural and thermodynamic studies with mutants of nuclease with buried ionizable groups at position 66 are sufficient to rule out contributions to the polarizability in the protein interior by some, but not all of these mechanisms. For example, the close similarity in the ionization behavior of Glu-66 and Lys-66, despite the very significant difference in the net charge of staphylococcal nuclease in the pH range where they titrate, suggests that fluctuations of surface ionizable groups do not contribute greatly to the high apparent polarizability at this deeply buried location (Simonson and Perahia, 1995; Simonson and Brooks, 1996; Smith et al., 1993). Another way in which high values of D_{app} have been rationalized previously is in terms of exposure of buried ionizable groups to solvent by global unfolding (Warshel, 1981; Warshel et al., 1984). In many of the proteins listed in a previously published survey of pK_a shifts of buried ionizable groups (García-Moreno et al., 1997), the size of the shift in pK_a is limited primarily by the free energy of unfolding of the host protein (Warshel, 1981). To avoid this problem the Glu-66 and Lys-66, mutations were introduced into constructs of nuclease that have been engineered specifically for greatly enhanced stability. The values of D_{app} that were measured in these mutants do not reflect global unfolding of the protein. The pK_a of Lys-66 in three different forms of staphylococcal nuclease with global stability (pH 7, 25°C) ranging from 5.7 to 12 kcal/mol are almost identical (García-Moreno et al., 1997; Stites et al., 1991), demonstrating that the pK_a does not simply report the acid unfolding of the protein. In the case of the V66E mutant, the acid/base titrations, chemical denaturation, and the proton titration curves also suggest that the magnitude of the pK_a shifts is not limited by the unfolding of the protein. PHS/V66E is highly destabilized when the buried group becomes ionized, but, as demonstrated by the data in Figs. 1, 2, and 3, approximately 85% of PHS/V66E remains folded even after the buried Glu is 90% ionized.

The structures of PHS/V66E constitute compelling evidence that exposure of buried ionizable groups to water molecules can be achieved through penetration into the core rather than by unfolding. The structures at pH 6 and 8 demonstrate that the buried Glu-66 is hydrated when the structure is in the native state. Note that the stability of PHS/V66E at 25°C in pH 6 (~5 kcal/mol) is almost the same as that of wild type nuclease (~5.4 kcal/mol) (Fig. 2). The water molecules were present in both PHS/V66E structures, suggesting that the waters that were in the structure at pH 8 did not penetrate because of the protein's lower global stability and higher propensity toward denaturation at this pH. The similarity between the polarizability reported by acidic and basic side chains at position 66 is consistent with the ascribed role of water as a general source of polarizability inside proteins.

Buried water molecules are common in light-activated and other membrane proteins, where they are usually found in association with buried ionizable groups (Deisenhofer and Michel, 1989; Luecke et al., 1998; Pebay-Peyroula, 1997). They are often part of intricate hydrogen-bonded networks that have evolved to harness the energy stored in buried ionizable groups for purposes of energy transduction and H^+ and e^- transfer. Buried water molecules have also been found in many water soluble, globular proteins where their acknowledged role is structural or enzymatic. Deeper understanding of the structural and energetic consequences of solvent penetration and its effect on pK_a values of buried ionizable groups is essential for improved understanding of structure–energy relationship in these systems. The experimental results reported in this paper contribute toward this end at several levels. First, they demonstrate that solvent penetration and organization of solvent in the hydrophobic core can take place without any significant global or local conformational rearrangements. Second, they suggest that solvent penetration must be treated explicitly in calculations of dielectric effects in the protein interior from first principles. Third, they provide useful estimates of the apparent dielectric constants that should be used with continuum methods to improve their ability to capture quantitatively the energetics of buried ionizable groups. Finally, they provide a set of pK_a values of buried ionizable groups that constitute essential benchmarks needed for the testing and

calibration of theoretical models for calculation of electrostatic energies.

We thank Prof. David Shortle for sharing his clones of PHS nuclease with us, and Dr. George Privalov from Applied Thermodynamics for his gift of the MOLE program for calculation of packing densities. We also thank Mr. Jack Aviv, Mr. Mike Smith, and Dr. Glen Ramsay of Aviv Instruments, Inc. for their invaluable contributions toward the automatization of denaturation and titration experiments.

This work was supported by National Science Foundation grant MCB-9600991 to B. G. M. E., and National Institutes of Health grant GM-52714 to W. E. S

REFERENCES

Antosiewicz, J., J. A. McCammon, and M. K. Gilson. 1994. Prediction of pH-dependent properties of proteins. *J. Mol. Biol.* 238:415–436.

Bone, S., and R. Pethig. 1982. Dielectric studies of the binding of water to lysozyme. *J. Mol. Biol.* 57:571–575.

Bone, S., and R. Pethig. 1985. Dielectric studies of protein hydration and hydration- induced flexibility. *J. Mol. Biol.* 181:323–326.

Buckle, A. M., P. Cramer, and A. R. Fersht. 1996. Structural and energetic responses to cavity-creating mutations in hydrophobic cores: observation of a water molecule and the hydrophilic nature of such hydrophobic cavities. *Biochemistry.* 35:4298–4305.

Brünger, A. T., J. Kuriyan, and M. Karplus. 1987. Crystallographic R factor refinement by molecular dynamics. *Science.* 235:458–460.

Brünger, A. T. 1992. X-PLOR Ver. 3.1. Yale University Press, New Haven, CT.

Churg, A. K., and A. Warshel. 1986. Control of the redox potential of cytochrome-c and microscopic dielectric effects in proteins. *Biochemistry.* 25:1675–1681.

Collins, K. D. 1997. Charge density-dependent strength of hydration and biological structure. *Biophys. J.* 72:65–76.

Dao-pin, S., D. E. Anderson, W. A. Baase, F. W. Dahlquist, and B. W. Matthews. 1991. Structural and thermodynamic consequences of burying a charged residue within the hydrophobic core of T4 lysozyme. *Biochemistry.* 30:11521–11529.

Deisenhofer, J., and H. Michel. 1989. The photosynthetic reaction center from the purple bacterium *Rhodopseudomonas viridis*. *EMBO J.* 8:2149–2170.

Denisov, V. P., B. Halle, J. Peters, and H. D. Hörlein. 1995. Residence times of the buried water molecules in bovine pancreatic trypsin inhibitor and its G36S mutant. *Biochemistry.* 34:9046–9051.

Denisov, V., J. Peters, H. D. Hörlein, and B. Halle. 1996. Using buried water molecules to explore the energy landscape of proteins. *Nature. Struc. Biol.* 3:505–509.

Ermler, U., G. Fritzsch, S. K. Buchanan, and H. Michel. 1994. Structure of the photosynthetic reaction centre from *Rhodobacter sphaeroides* at 2.65 Å resolution: cofactors and protein–cofactor interactions. *Structure.* 2:925–936.

Ernst, J. A., R. T. Clubb, H. Zhou, A. M. Gronenborn, and G. M. Clore. 1995. Demonstration of positionally disordered water within a protein hydrophobic cavity by NMR. *Science.* 267:1813–1817.

Feher, V. A., E. P. Baldwin, and F. W. Dahlquist. 1996. Access of ligands to cavities within the core of a protein is rapid. *Nature Struct. Biol.* 3:516–521.

García, A. E., and G. Hummer. 2000. Water penetration and escape in proteins. *Proteins: Struc. Funct. Gen.* 38:261–272.

García-Moreno E., B., J. J. Dwyer, A. G. Gittis, E. E. Lattman, D. S. Spencer, and W. E. Stites. 1997. Experimental measurement of the effective dielectric constant in the hydrophobic core of a protein. *Biophys. Chem.* 64:212–224.

Gibas, C. J., and S. Subramanian. 1996. Explicit solvent models in protein pK_a calculations. *Biophys. J.* 71:138–147.

Giletto, A., and C. N. Pace. 1999. Buried, charged, non ion-paired aspartic acid 76 contributes favorably to the conformational stability of ribonuclease T1. *Biochemistry.* 8:13379–13384.

Gilson, M. K., and B. H. Honig. 1986. The dielectric constant of a folded protein. *Biopolymers.* 25:2097–2119.

Gregg, E. C. 1976. Dielectric Constants of Solids. In Handbook of Chemistry and Physics. Chemical Rubber Company, Cleveland, OH. E55–E60.

Harvey, S. C., and P. Hoekstra. 1972. Dielectric relaxation spectra of water adsorbed on lysozyme. *J. Phys. Chem.* 76:2987–2994.

Havranek, J. J., and P. B. Harbury. 1999. Tanford-Kirkwood electrostatics for protein modeling. *Proc. Natl. Acad. Sci. USA.* 96:11145–11150.

King, G., F. S. Lee, and A. Warshel. 1991. Microscopic simulations of macroscopic dielectric constants of solvated proteins. *J. Chem. Phys.* 95:4366–4377.

Kraulis, P. 1991. MOLSCRIPT: a program to produce both detailed and schematic plots of proteins. *J. Appl. Crystl.* 24:946–950.

Liu, K., M. G. Brown, J. D. Cruzan, and R. J. Saykally. 1996. Vibration-rotation tunneling spectra of the water pentamer: structure and dynamics. *Science.* 271:62–64.

Löffler, G., H. Schreiber, and O. Steinhauser. 1997. Calculation of the dielectric properties of a protein and its solvent: theory and a case study. *J. Mol. Biol.* 270:520–534.

Luecke, J., H. T. Richter, and J. K. Lanyi. 1998. Proton transfer pathways in bacteriorhodopsin at 2.3 angstrom resolution. *Science.* 280: 1934–1937.

Matthew, J. B., F. R. N. Gurd, B. García-Moreno E., M. A. Flanagan, K. L. March, and S. J. Shire. 1985. pH-dependent processes in proteins. *CRC Crit. Rev. Biochem.* 18:91–189.

Martinez, S. E., D. Huang, M. Ponomarev, W. A. Cramer, and J. L. Smith. 1996. The heme redox center of chloroplast cytochrome *f* is linked to a buried five-water chain. *Protein Sci.* 5:1081–1092.

Merrit, E. A., and D. J. Bacon. 1997. Raster 3D: photorealistic molecular graphics. *Methods Enzymol.* 277:505–524.

Meyer, E. 1992. Internal water molecules and H-bonding in biological macromolecules: a review of structural features with functional implications. *Protein Sci.* 1:1543–1562.

Oprea, T. I., G. Hummer, and A. E. García. 1997. Identification of a functional water channel in cytochrome P450 enzymes. *Proc. Natl. Acad. Sci. USA.* 94:2133–2138.

Ormö, M., A. Cubitt, K. Kallio, L. A. Gross, R. Y. Tsien, and S. J. Remington. 1996. Crystal structure of the *Aequorea victoria* green fluorescent protein. *Science.* 273:1392–1395.

Otting, G., E. Liepinsh, and K. Wüthrich. 1991. Protein hydration in aqueous solution. *Science.* 254:974–980.

Otting, G., E. Liepinish, B. Halle, and U. Frey. 1997. NMR identification of hydrophobic cavities with low water occupancies in protein structures using small gas molecules. *Nature Struct. Biol.* 4:396–404.

Pebay-Peyroula, E., G. Rummel, J. P. Rosenbusch, and E. M. Landau. 1997. X-ray structure of bacteriorhodopsin at 2.5 angstroms from microcrystals grown in lipidic cubic phases. *Science.* 277:1676–1681.

Pethig, R. 1979. Dielectric and electronic properties of biological materials. Wiley, New York. 139.

Privalov, G. 1995. Packing of protein interior: structure and distribution of packing density. Ph.D. Dissertation, Johns Hopkins University, Baltimore, MD.

Roe, S. M., and M. M. Teeter. 1993. Patterns for prediction of hydration around polar residues in proteins. *J. Mol. Biol.* 229:419–427.

Rose, G., W. B. Young, and L. M. Gierasch. 1983. Interior turns in globular proteins. *Nature.* 304:655–657.

Sack, J. S. 1988. CHAIN—crystallographic modeling program. *J. Molec. Graphics.* 6:224–225.

Sack, J. S. 1993. CHAIN Ver. 5.4. Baylor College of Medicine, Houston, TX.

Sharp, K., and B. Honig. 1990. Electrostatic interactions in macromolecules: theory and applications. *Annu. Rev. Biophys. Biophys. Chem.* 19:301–332.

Shih, P., D. R. Holland, and J. F. Kirsch. 1995. Thermal stability determinants of chicken egg-white lysozyme core mutants: hydrophobicity, packing volumes, and conserved buried water molecules. *Protein Sci.* 4:2050–2062.

Shortle, D., and A. K. Meeker. 1986. Mutant forms of staphylococcal nuclease with altered patterns of guanidine hydrochloride and urea denaturation. *Proteins: Struc. Funct. Gen.* 1:81–89.

Simonson, T., and C. L. Brooks, III. 1996. Charge screening and the dielectric constant of proteins: insights from molecular dynamics. *J. Am. Chem. Soc.* 118:8452–8458.

Simonson, T., and D. Perahia. 1995. Internal and interfacial dielectric properties of cytochrome c from molecular dynamics in aqueous solution. *Proc. Natl. Acad. Sci. USA.* 92:1082–1086.

Smith, P. E., R. M. Brunne, A. E. Mark, and W. F. van Gunsteren. 1993. Dielectric properties of trypsin inhibitor and lysozyme calculated from molecular dynamics simulations. *J. Phys. Chem.* 97:2009–2014.

Sreenivasan, U., and P. H. Axelsen. 1992. Buried water in homologous serine proteases. *Biochemistry.* 31:12785–12791.

Stites, W. E., M. P. Byrne, J. Aviv, M. Kaplan, and P. M. Curtis. 1995. Instrumentation for automated determination of protein stability. *Anal. Biochem.* 227:112–122.

Stites, W. E., A. G. Gittis, E. E. Lattman, and D. Shortle. 1991. In a staphylococcal nuclease mutant the side-chain of a lysine replacing valine 66 is fully buried in the hydrophobic core. *J. Mol. Biol.* 221:7–14.

Teeter, M. M. 1984. Water structure of a hydrophobic protein at atomic resolution: pentagon rings of water molecules in crystals of crambin. *Proc. Natl. Acad. Sci. USA.* 81:6014–6018.

Thanki, N., J. M. Thornton, and J. M. Goodfellow. 1988. Distribution of water around amino acid residues in proteins. *J. Mol. Biol.* 202: 637–657.

Tüchsen, E., J. M. Hayes, S. Ramaprasad, V. Copie, and C. Woodward. 1987. Solvent exchange of buried water and hydrogen exchange of peptide NH groups hydrogen bonded to buried waters in bovine pancreatic trypsin inhibitor. *Biochemistry.* 26:5163–5172.

Warshel, A. 1978. Energetics of enzyme catalysis. *Proc. Natl. Acad. Sci. USA.* 75:5250–5254.

Warshel, A. 1981. Calculations of enzyme reactions: calculations of pK_a, proton transfer reactions, and general acid catalysis reactions in enzymes. *Biochemistry.* 20:3167–3177.

Warshel, A., and J. Åqvist. 1991. Electrostatic energy and macromolecular function. *Annu. Rev. Biophys. Biophys. Chem.* 20:267–298.

Warshel, A., J. Åqvist, and S. Creighton. 1989. Enzymes work by desolvation substitution rather than by desolvation. *Proc. Natl. Acad. Sci. USA.* 86:5820–5824.

Warshel, A., A. Papayzan, and I. Muegge. 1997. Microscopic and semimicroscopic redox calculations: what can and cannot be learned from continuum models. *JBIC.* 2:143–152.

Warshel, A., S. T. Russell, and A. K. Churg. 1984. Macroscopic models for studies of electrostatic interactions in proteins: limitations and applicability. *Proc. Natl. Acad. Sci. USA.* 81:4785–4789.

Williams, M. A., J. M. Goodfellow, and J. M. Thornton. 1994. Buried waters and internal cavities in monomeric proteins. *Protein Sci.* 3:1224–1235.

Wimley, W. C., T. P. Creamer, and S. J. White. 1996. Solvation energies of amino acid side chains and backbone in a family of host–guest pentapeptides. *Biochemistry.* 35:5109–5124.

Woodward, C., I. Simon, and E. Tüchsen. 1982. Hydrogen exchange and the dynamic structure of proteins. *Mol. Cell. Biochem.* 48:135–160.